

Supporting Information

Study on Importance of Uniformity and Nanoparticle Size of ZIF-8 Carbon Nanoarchitecture for Enhancing Electrochemical Property

Donggyun Kim^a, Jinhyeon Park^a, Seonghyeon Jung,^a Jieun Jang^a, Minsu Han^b, Minjun Kim^b, Wenkai Zhu^c, Woo-Jin Song^d, Yusuke Yamauchi^b, Jeonghun Kim^{a*}

^a Department of Chemical and Biomolecular Engineering, Yonsei University, Seoul 03722, Republic of Korea

^b Australian Institute for Bioengineering and Nanotechnology (AIBN), The University of Queensland, Brisbane, Queensland 4072, Australia

^c College of Chemistry and Materials Engineering, Zhejiang A&F University, Hangzhou 311300, China

^d Department of Organic Materials Engineering, Chungnam National University, 99 Daehak-ro, Yuseong-gu, Daejeon, 34134 Republic of Korea

* Corresponding author.

E-mail address: jhkim03@yonsei.ac.kr (Jeonghun Kim)

Table S1. Summary of the synthesis conditions for all samples.

| Samples | Zn(OAc) ₂ (g) | 2-mIm (g) | Water content (mL) | Pouring time (s) | Pour order | Stirring |
|----------|-----------------------------|--------------|--------------------------|------------------------|-------------|----------|
| ZIF-8-m1 | | 6.73 | 25 | 30 | Zn to 2-mIm | 750 rpm |
| ZIF-8-m2 | | 6.73 | 25 | 3 | Zn to 2-mIm | 750 rpm |
| ZIF-8-m3 | 1.5 | 6.73 | 25 | 1 | Zn to 2-mIm | 750 rpm |
| ZIF-8-m4 | | 6.73 | 35 | 1 | Zn to 2-mIm | 750 rpm |
| ZIF-8-m5 | | 5.21 | 25 | 1 | Zn to 2-mIm | 750 rpm |
| ZIF-8-n | | 6.73 | 25 | 1 | 2-mIm to Zn | 200 rpm |

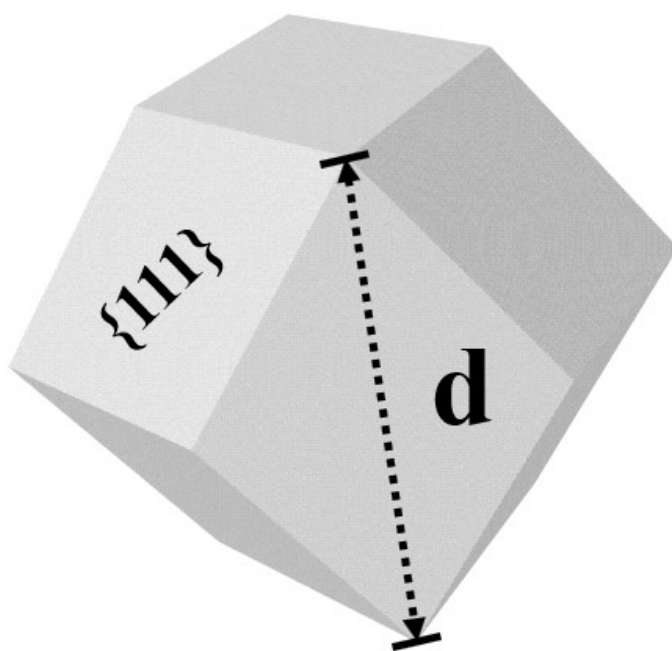


Figure S1. Schematic illustration of the measurement of the size (d) of the ZIF-8 particle with a rhombic dodecahedron shape.

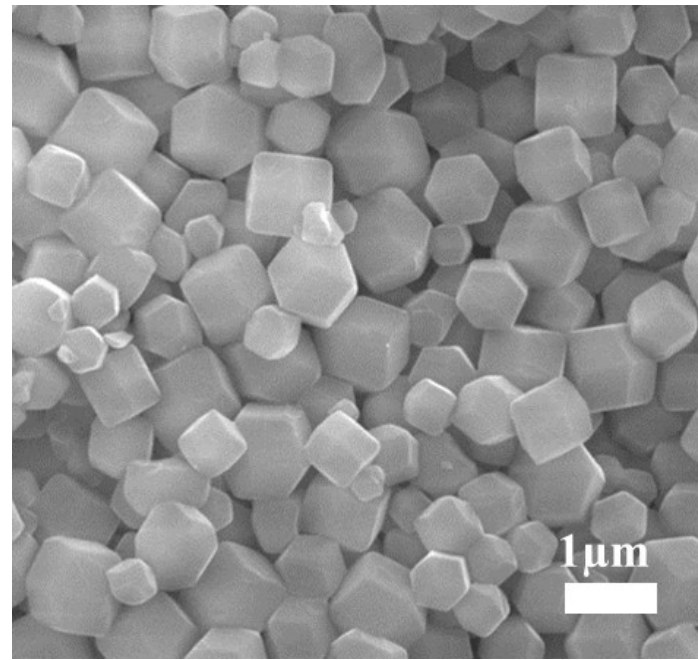


Figure S2. Scanning electron microscopy (SEM) images of ZIF-8-n.

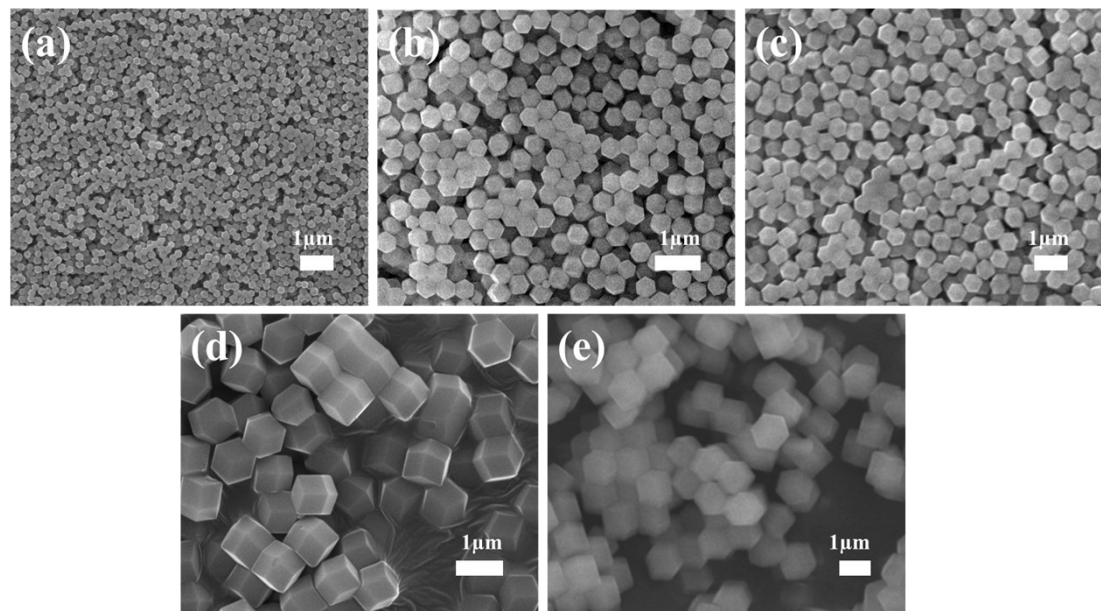


Figure S3. SEM images of (a) ZIF-8-m1, (b) ZIF-8-m2, (c) ZIF-8-m3, (d) ZIF-8-m4, and (e) ZIF-8-m5.

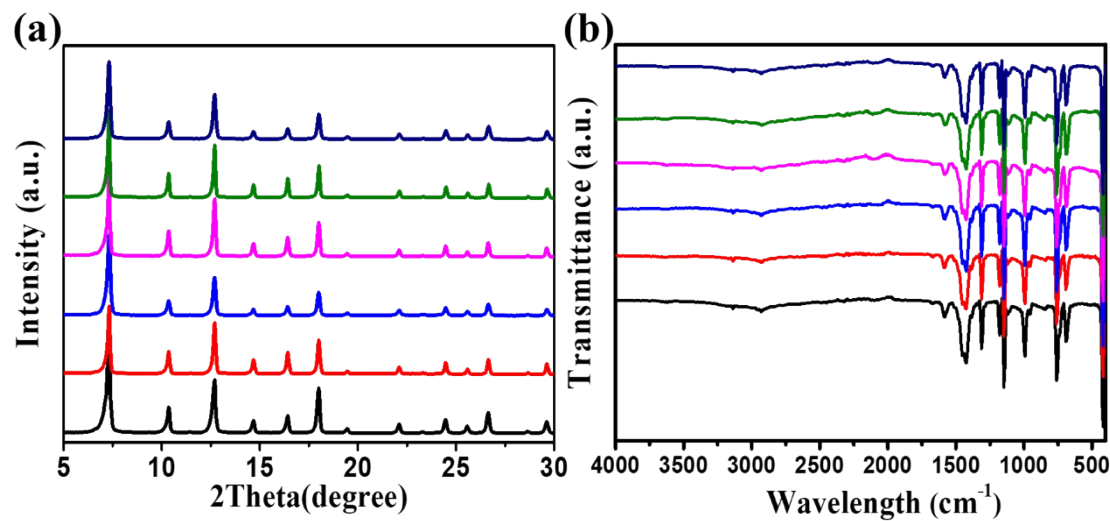


Figure S4. (a) X-ray diffraction (XRD) patterns and (b) Fourier transform infrared (FT-IR) spectra (Black: ZIF-8-m1, Red: ZIF-8-m2, Blue: ZIF-8-m3, Pink: ZIF-8-m4, Green: ZIF-8-m5, Navy: ZIF-8-n).

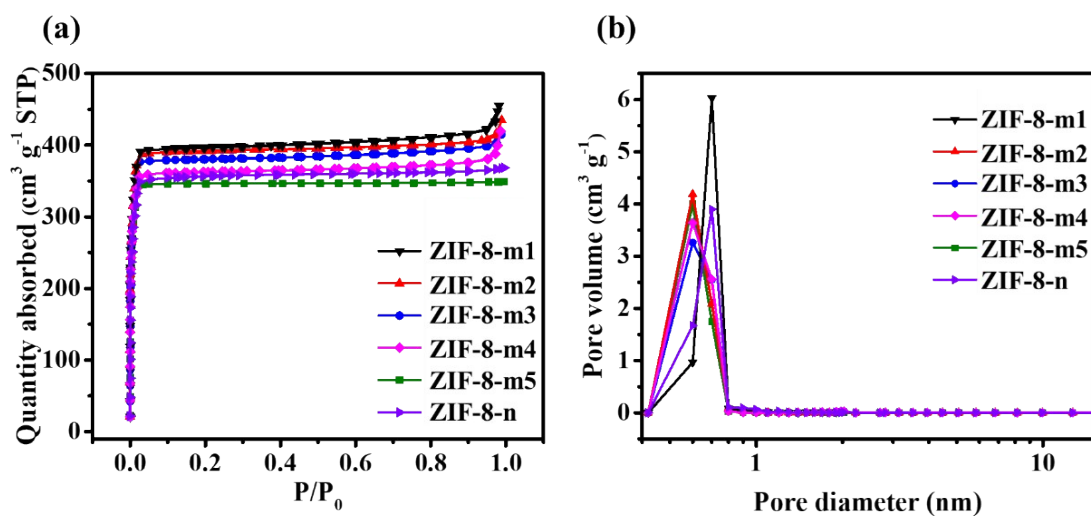


Figure S5. (a) N_2 adsorption–desorption isotherms, and (b) pore size distribution of the ZIF-8 samples.

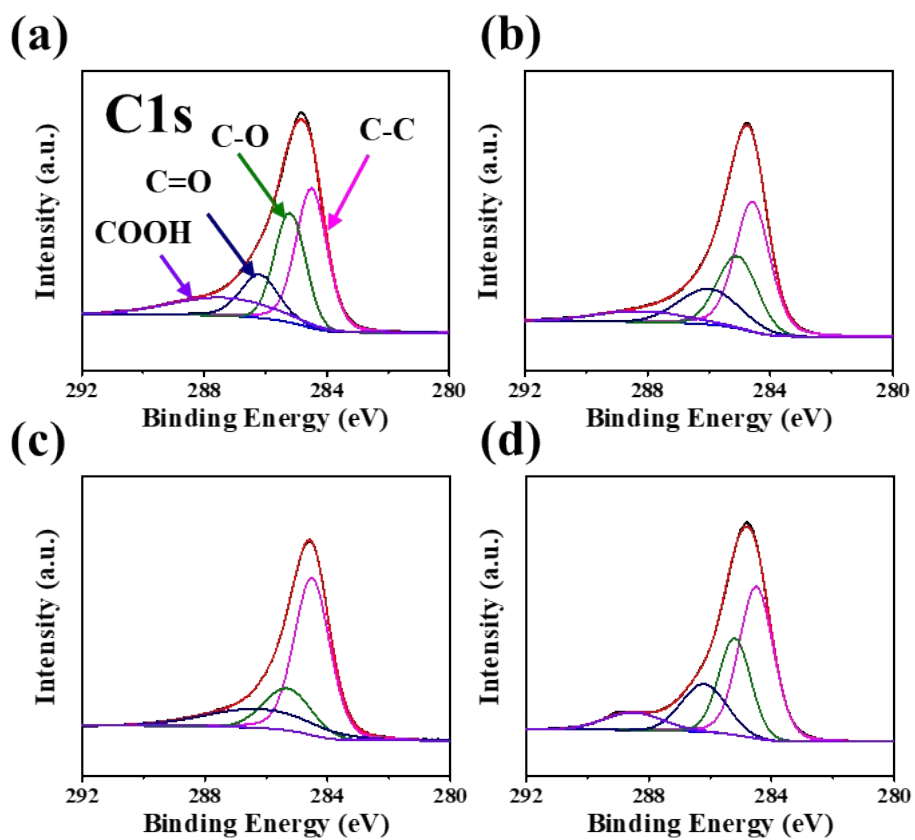


Figure S6. X-ray photoelectron spectroscopy (XPS) profiles of the C1s of (a) ZIF-8-C-m2, (b) ZIF-8-C-m3, (c) ZIF-8-C-m4, and (d) ZIF-8-C-m5.

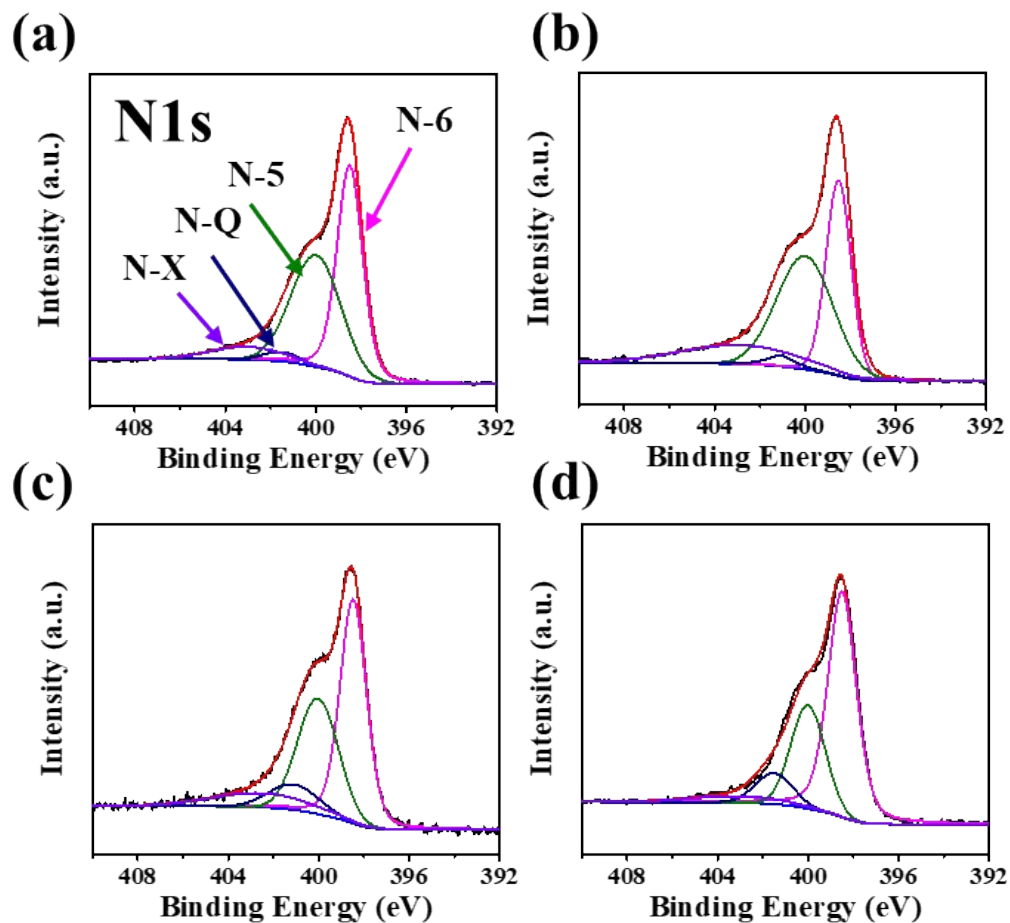


Figure S7. N1s XPS profiles of: (a) ZIF-8-C-m2, (b) ZIF-8-C-m3, (c) ZIF-8-C-m4, and (d) ZIF-8-C-m5.

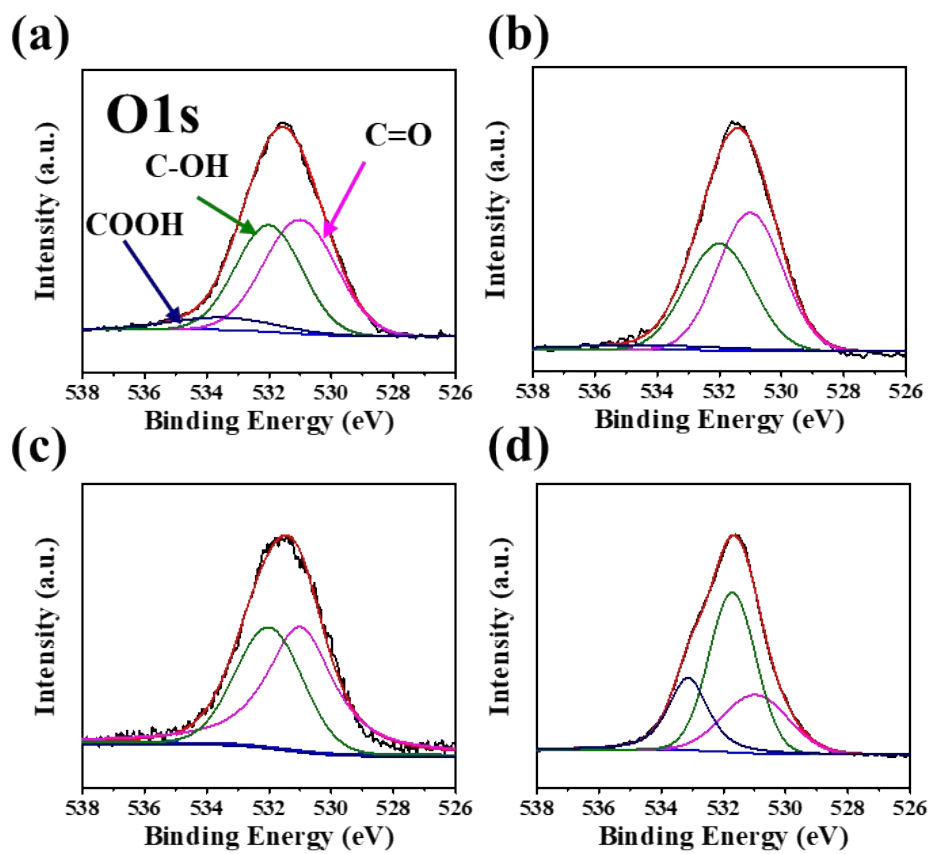


Figure S8. O1s XPS profiles of: (a) ZIF-8-C-m2, (b) ZIF-8-C-m3, (c) ZIF-8-C-m4, and (d) ZIF-8-C-m5.

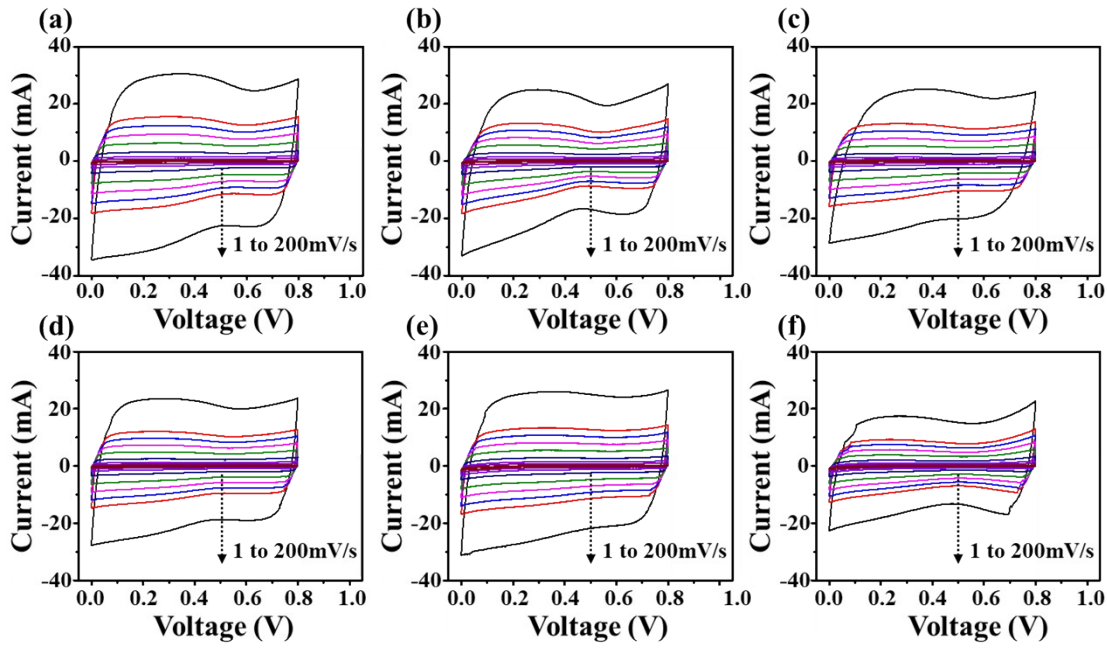


Figure S9. Cyclic voltammetry (CV) curves of (a): ZIF-8-C-m1 (b): ZIF-8-C-m2, (c): ZIF-8-C-m3, (d): ZIF-8-C-m4, (e): ZIF-8-C-m5, (f): ZIF-8-C-n at 1, 2, 5, 10, 20, 40, 60, 80, 100, and 200 mV s⁻¹.

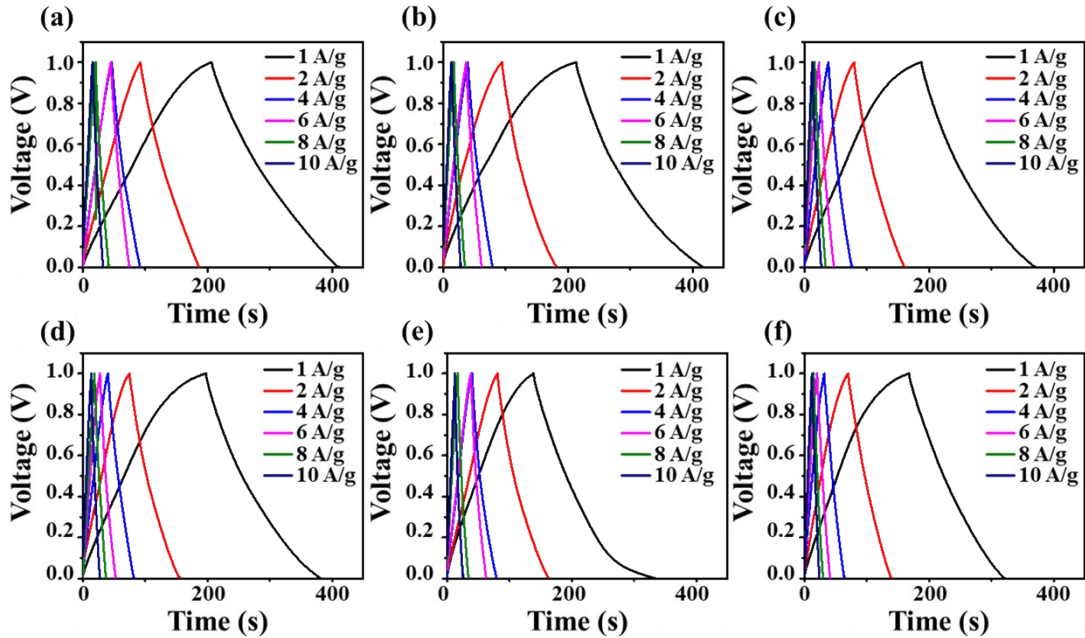


Figure S10. CV and galvanostatic charge–discharge (GCD) curves of: (a) ZIF-8-C-m1, (b) ZIF-8-C-m2, (c) ZIF-8-C-m3, (d) ZIF-8-C-m4, (e) ZIF-8-C-m5, and (f) ZIF-8-C-n at 1, 2, 4, 6, 8, 10 A g⁻¹.

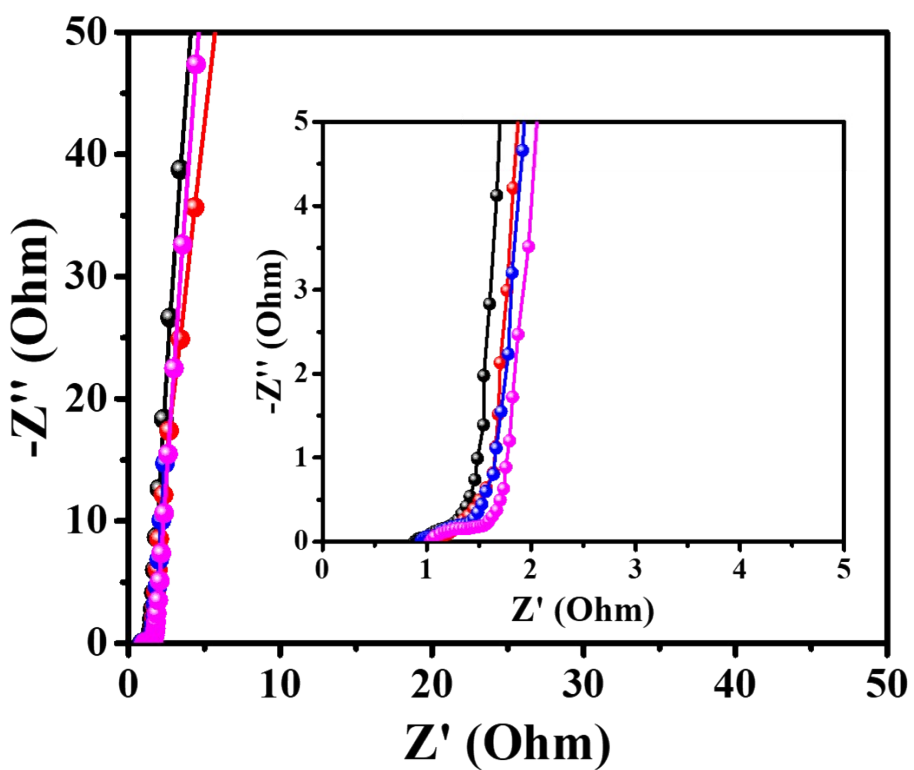


Figure S11. Nyquist plots of ZIF-8-C-m2 (black), ZIF-8-C-m3 (red), ZIF-8-C-m4 (blue), and ZIF-8-C-m5 (pink).

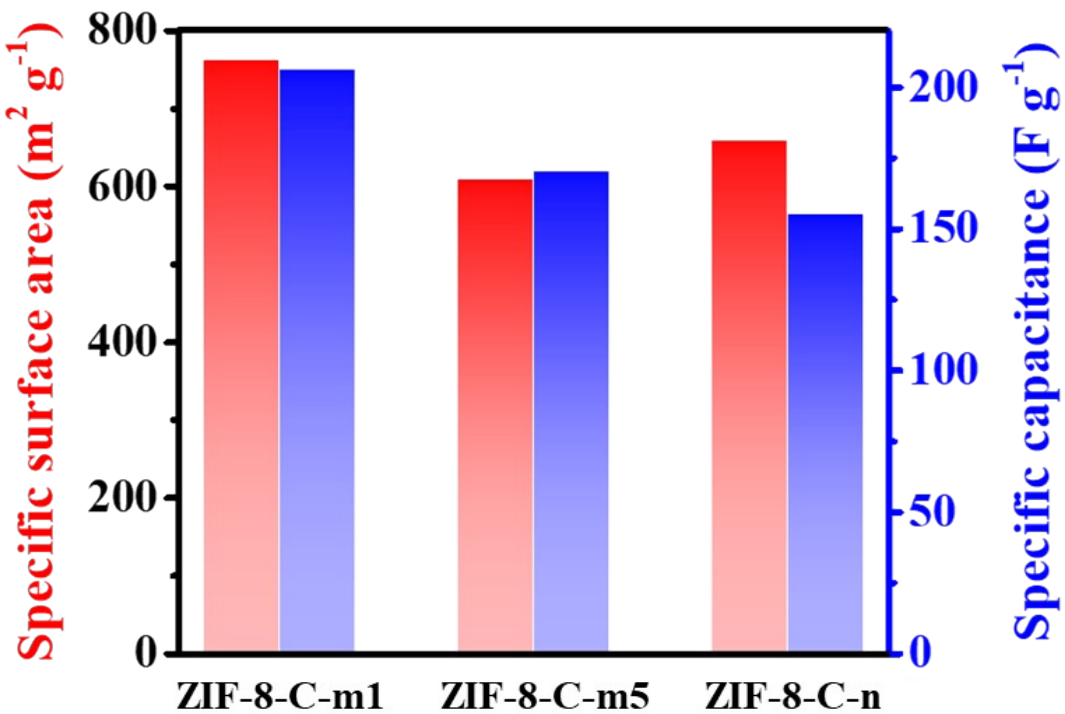


Figure S12. Comparison of the relative specific surface area and specific capacitance of ZIF-8-C-m1, ZIF-8-C-m5, and other ZIF-8-C-n samples.

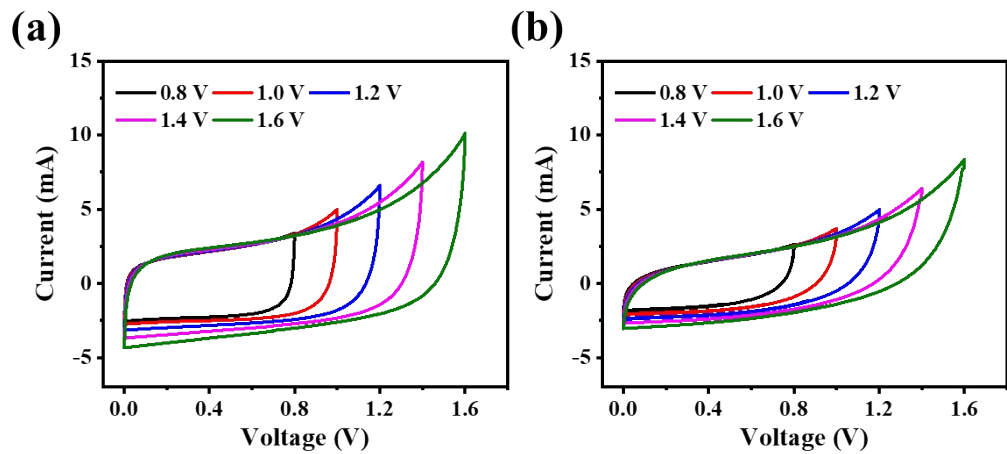


Figure S13. CV curves at $50 \text{ mV}\cdot\text{s}^{-1}$ under different voltage windows of ZIF-8-C-m5, and ZIF-8-C-n in the two-electrode system.

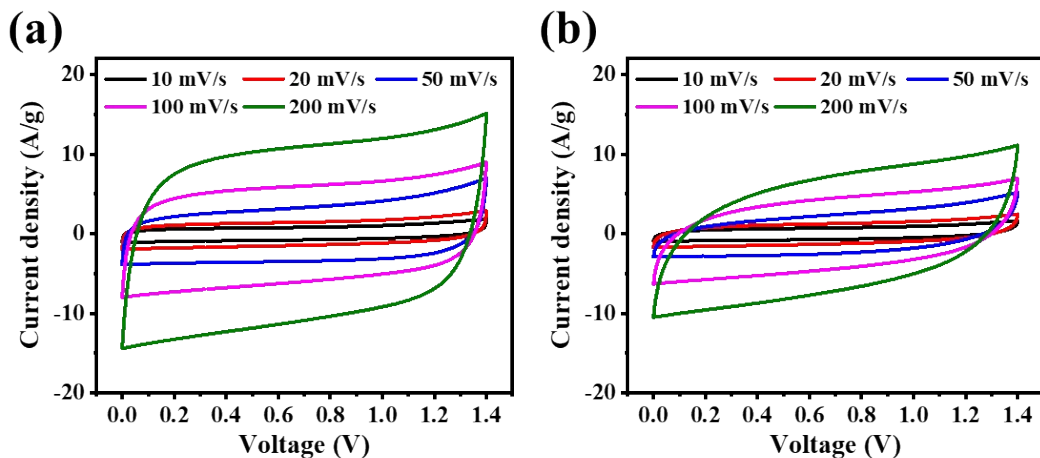


Figure S14. CV curves at different scan rates from 10 to $200 \text{ mV}\cdot\text{s}^{-1}$ of ZIF-8-C-m5, and ZIF-8-C-n in the two-electrode system.

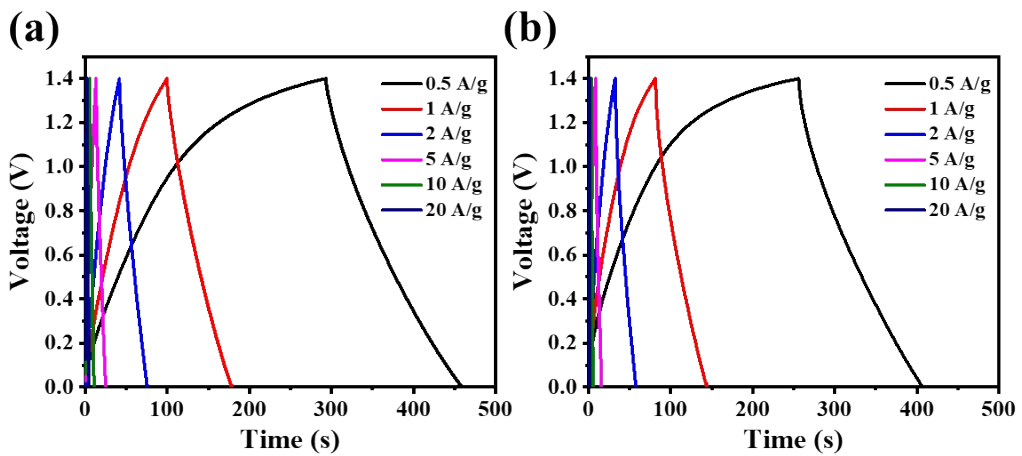


Figure S15. GCD curves at various current densities ($0.5\text{--}20\text{ A}\cdot\text{g}^{-1}$) of ZIF-8-C-m5, and ZIF-8-C-n in the two-electrode system.

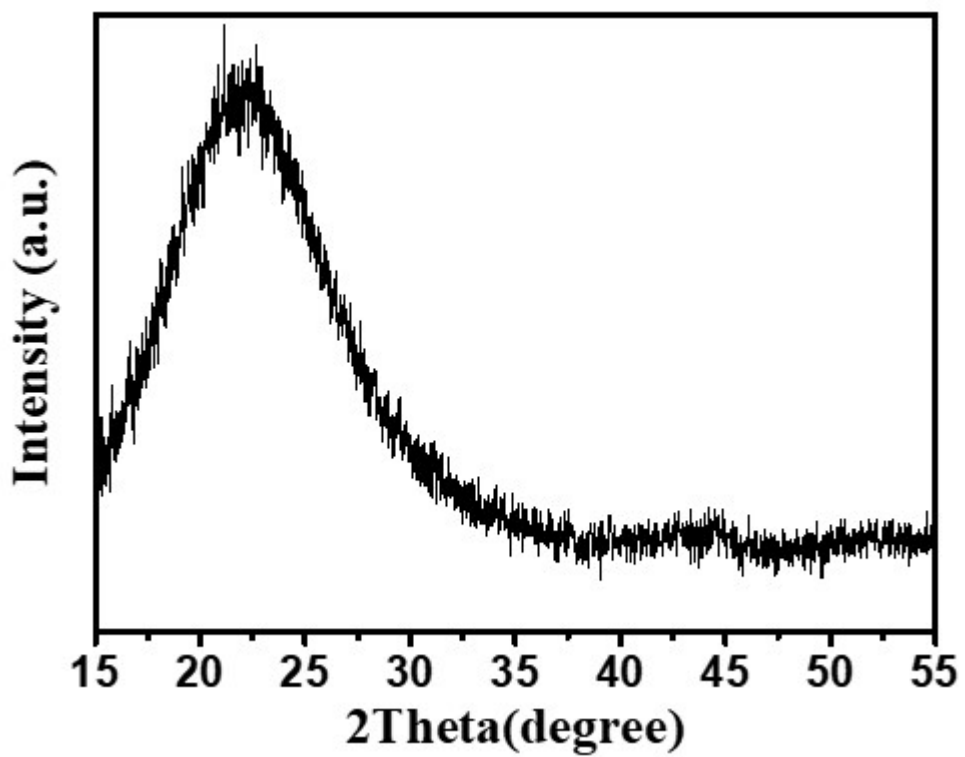


Figure S16. Ex-situ XRD patterns of ZIF-8-C-m1 after 10,000 cycle stability test in the flexible symmetric device system.

Table S2. Results of the BET analysis of the ZIF-8-derived carbon with different particle sizes.

| Sample | S _{bet} (m ² /g) | V _{total} (cm ³ /g) | V _{micro} (cm ³ /g) | D _{avg} (nm) |
|----------|--------------------------------------|---|---|-----------------------|
| ZIF-8-m1 | 1206.5 | 0.7039 | 0.5998 | 1.27 |
| ZIF-8-m2 | 1119.2 | 0.6325 | 0.5627 | 1.14 |
| ZIF-8-m3 | 1110.1 | 0.6249 | 0.5729 | 1.10 |
| ZIF-8-m4 | 1092 | 0.6021 | 0.5539 | 1.24 |
| ZIF-8-m5 | 1040.2 | 0.5926 | 0.5793 | 1.11 |
| ZIF-8-n | 1073.2 | 0.5821 | 0.5402 | 1.14 |

Table S3. XPS data of the ZIF-8 and ZIF-8-C samples.

| Sample | C (at%) | N (at%) | O (at%) | Zn (at%) |
|------------|---------|---------|---------|----------|
| ZIF-8-m1 | 62.11 | 27.89 | 1.29 | 8.71 |
| ZIF-8-C-m1 | 76.93 | 16.11 | 6.96 | - |
| ZIF-8-C-m2 | 78.6 | 15.77 | 5.63 | - |
| ZIF-8-C-m3 | 81.15 | 12.77 | 6.08 | - |
| ZIF-8-C-m4 | 81.13 | 12.91 | 5.96 | - |
| ZIF-8-C-m5 | 81.5 | 11.31 | 7.19 | - |
| ZIF-8-C-n | 79.22 | 11.31 | 9.47 | - |

Table S4. Specific capacitance (F g^{-1}) of the ZIF-8-C samples calculated from the CV curves obtained at different scan rates.

| Scan rate (mV s^{-1}) | ZIF-8-C-m1 | ZIF-8-C-m2 | ZIF-8-C-m3 | ZIF-8-C-m4 | ZIF-8-C-m5 | ZIF-8-C-n |
|--|------------|------------|------------|------------|------------|-----------|
| 1 | 178.47 | 156.56 | 164.14 | 150.48 | 140.53 | 112.02 |
| 5 | 165.28 | 143.39 | 142.47 | 138.31 | 130.21 | 109.12 |
| 10 | 162.36 | 140.43 | 137.57 | 136.68 | 129.60 | 107.43 |
| 20 | 158.21 | 134.47 | 133.25 | 132.72 | 126.12 | 103.33 |
| 40 | 153.13 | 127.68 | 128.47 | 127.72 | 122.07 | 98.14 |
| 60 | 149.43 | 122.94 | 125.31 | 124.13 | 119.26 | 94.73 |
| 80 | 146.31 | 119.24 | 122.77 | 121.37 | 116.96 | 91.96 |
| 100 | 143.64 | 116.15 | 120.52 | 118.79 | 114.99 | 89.65 |
| 200 | 132.54 | 103.97 | 111.12 | 100.91 | 107.19 | 80.37 |

Table S5. Specific capacitance (F g^{-1}) of the ZIF-8-C samples calculated from the GCD curves at different current densities.

| Current densities (A g^{-1}) | ZIF-8-C-m1 | ZIF-8-C-m2 | ZIF-8-C-m3 | ZIF-8-C-m4 | ZIF-8-C-m5 | ZIF-8-C-n |
|--|------------|------------|------------|------------|------------|-----------|
| 1 | 206.4 | 201.54 | 196.54 | 193 | 183.27 | 155.34 |
| 2 | 188.02 | 189.01 | 172.73 | 173.36 | 150.52 | 142.2 |
| 4 | 180.18 | 170.89 | 163.64 | 166.72 | 139.71 | 131.32 |
| 6 | 175.38 | 158.91 | 160.53 | 151.1 | 132.54 | 124.26 |
| 8 | 168.8 | 152.19 | 146.49 | 146.2 | 130.87 | 120 |
| 10 | 165.6 | 149 | 142.3 | 138.8 | 125.42 | 117.8 |

Table S6. Series resistance (R_s) and charge transfer resistance (R_{ct}) of ZIF-8-C samples estimated from the Nyquist plot.

| | ZIF-8-C-m1 | ZIF-8-C-m2 | ZIF-8-C-m3 | ZIF-8-C-m4 | ZIF-8-C-m5 | ZIF-8-C-n |
|-----------------------|------------|------------|------------|------------|------------|-----------|
| R_s (Ω) | 0.9145 | 0.93405 | 0.97758 | 0.95804 | 1.0376 | 1.0253 |
| R_{ct} (Ω) | 0.2124 | 0.2323 | 0.2334 | 0.4187 | 0.493 | 0.5718 |

Table S7. Comparison of the specific capacitance of various previously reported ZIF-8-derived carbon materials for supercapacitors.

| Samples | Specific capacitance (F·g ⁻¹) | Current density (A·g ⁻¹) | Cycle number | Capacitance retention (%) | Particle size (nm) | Power density (W·kg ⁻¹) | Energy density (Wh·kg ⁻¹) | Ref |
|------------------|--|---|---------------|---------------------------|--------------------|-------------------------------------|---------------------------------------|----------|
| MPC | 148.4 | 2 | - | - | 85 | - | - | 1 |
| CNT@CZIF-1 | 168 | 0.5 | 1,000 | 86.40 | 20 | - | - | 2 |
| C-ZIF-8 | 155.9 | 1 | 10,000 | 95.5 | 50 | - | - | 3 |
| NCGs | 225 | 0.5 | 10,000 | 96.60 | 50 | 447 | 12.7 | 4 |
| C(ZIF-8) | 130 | 1 | - | - | 100 | - | - | 5 |
| PC-900 | 173 | 1 | - | - | 150 | 650 | 7.5 | 6 |
| NPC | 184.4 | 1 | - | - | 200 | - | - | 7 |
| N-HPC-900 | 182.5 | 0.2 | 5,000 | 94.79 | 200 | 50 | 4.46 | 8 |
| ZPC-900 | 185.9 | 1 | - | - | 800 | - | - | 9 |
| HPC NPs | 134.5 | 1 | 10,000 | 90.70 | 480 | - | - | 10 |
| Assy-ZIF-8-DC | 170 | 1 | 60,000 | 96.00 | 110 | 105 | 5.9 | 11 |
| ZIF-8/GO | 95 | 1 | - | - | 500 | - | - | 12 |
| This work | 206.4 | 1 | 10,000 | 99.65 | 147 | 350 | 19.4 | - |

References

1. M. Kim, X. Xu, R. Xin, J. Earnshaw, A. Ashok, J. Kim, T. Park, A. K. Nanjundan, W. A. El-Said and J. W. Yi, *ACS applied materials & interfaces*, 2021, **13**, 52034-52043.
2. L. Wan, E. Shamsaei, C. D. Easton, D. Yu, Y. Liang, X. Chen, Z. Abbasi, A. Akbari, X. Zhang and H. Wang, *Carbon*, 2017, **121**, 330-336.
3. Y. Wang, B. Chen, Y. Zhang, L. Fu, Y. Zhu, L. Zhang and Y. Wu, *Electrochimica Acta*, 2016, **213**, 260-269.
4. L. Wang, C. Wang, H. Wang, X. Jiao, Y. Ouyang, X. Xia, W. Lei and Q. Hao, *Electrochimica Acta*, 2018, **289**, 494-502.
5. H. Yu, W. Zhu, H. Zhou, J. Liu, Z. Yang, X. Hu and A. Yuan, *RSC advances*, 2019, **9**, 9577-9583.
6. H. Zhang, L. Fang, Y. Guo, Z. Wang, H. Hu, W. He and P. Wang, *Journal of Energy Storage*, 2024, **80**, 110138.
7. Z. Shang, X. An, S. Nie, N. Li, H. Cao, Z. Cheng, H. Liu, Y. Ni and L. Liu, *Journal of Bioresources and Bioproducts*, 2023, **8**, 292-305.
8. Z. Shang, X. An, L. Liu, J. Yang, W. Zhang, H. Dai, H. Cao, Q. Xu, H. Liu and Y. Ni, *Carbohydrate Polymers*, 2021, **251**, 117107.
9. C. Guo, G. Li, Y. Wu, X. Wang, Y. Niu and J. Wu, *Energies*, 2023, **16**, 7232.
10. Y. Long, X. An, H. Zhang, J. Yang, L. Liu, Z. Tian, G. Yang, Z. Cheng, H. Cao and H. Liu, *Chemical Engineering Journal*, 2023, **451**, 138877.
11. Y. Bu, W. Jiang, H. Zhang, Q. Kang, Y. Zhou, T. Sun, J. Lian, Q. Xu, M. Zhang and H. Zhuang, *Journal of Power Sources*, 2023, **563**, 232786.
12. W. Zhang, Y. Tan, Y. Gao, J. Wu, J. Hu, A. Stein and B. Tang, *Journal of Applied Electrochemistry*, 2016, **46**, 441-450.